Report

Current Biology

Monovision and the Misperception of Motion

Graphical Abstract

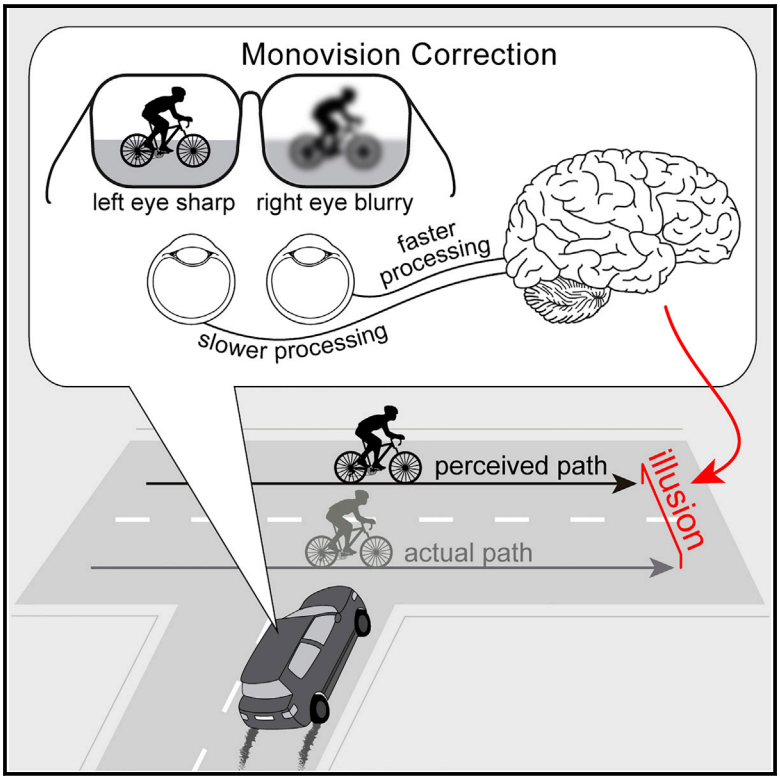

Authors

Johannes Burge,
Victor Rodriguez-Lopez,
Carlos Dorronsoro

Correspondence

jburge@psych.upenn.edu

In Brief

Burge et al. show that the interocular blur differences caused by a common prescription lens correction can cause dramatic misperceptions of motion. The illusions may impact public safety. The authors explain the illusion and demonstrate that appropriate combination of non-invasive ophthalmic interventions can eliminate the illusion.

Highlights

- Monovision induces interocular blur differences and a mismatch in processing speed
- The speed mismatch means a common lens correction can cause dramatic motion illusions
- Drivers may misperceive the distance of cyclists by the width of a narrow street lane
- Novel combinations of non-invasive ophthalmic interventions can abolish the illusion

Burge et al., 2019, Current Biology *29*, 2586–2592
August 5, 2019
https://doi.org/10.1016/j.cub.2019.06.070

CellPress

CellPress

Current Biology
Report

Monovision and the Misperception of Motion

Johannes Burge,[1,2,3,5,*] Victor Rodriguez-Lopez,[1,4] and Carlos Dorronsoro[4]
[1]Department of Psychology, University of Pennsylvania, Goddard 426, 3710 Hamilton Walk, Philadelphia, PA 19104, USA
[2]Neuroscience Graduate Group, University of Pennsylvania, Goddard 426, 3710 Hamilton Walk, Philadelphia, PA 19104, USA
[3]Bioengineering Graduate Group, University of Pennsylvania, Goddard 426, 3710 Hamilton Walk, Philadelphia, PA 19104, USA
[4]Institute of Optics, Spanish National Research Council, IO-CSIC, Calle Serrano 121, 28006 Madrid, Spain
[5]Lead Contact
*Correspondence: jburge@psych.upenn.edu
https://doi.org/10.1016/j.cub.2019.06.070

SUMMARY

Monovision is a common prescription lens correction for presbyopia [1]. Each eye is corrected for a different distance, causing one image to be blurrier than the other. Millions of people have monovision corrections, but little is known about how interocular blur differences affect motion perception. Here, we report that blur differences cause a previously unknown motion illusion that makes people dramatically misperceive the distance and three-dimensional direction of moving objects. The effect occurs because the blurry and sharp images are processed at different speeds. For moving objects, the mismatch in processing speed causes a neural disparity, which results in the misperceptions. A variant of a 100-year-old stereo-motion phenomenon called the Pulfrich effect [2], the illusion poses an apparent paradox: blur reduces contrast, and contrast reductions are known to cause neural processing delays [3–6], but our results indicate that blurry images are processed milliseconds more quickly. We resolve the paradox with known properties of the early visual system, show that the misperceptions can be severe enough to impact public safety, and demonstrate that the misperceptions can be eliminated with novel combinations of non-invasive ophthalmic interventions. The fact that substantial perceptual errors are caused by millisecond differences in processing speed highlights the exquisite temporal calibration required for accurate perceptual estimation. The motion illusion—the reverse Pulfrich effect—and the paradigm we use to measure it should help reveal how optical and image properties impact temporal processing, an important but understudied issue in vision and visual neuroscience.

RESULTS AND DISCUSSION

In the year 2020, nearly two billion people will have presbyopia worldwide [7]. Presbyopia is the age-related loss of focusing ability due to the stiffening of the crystalline lens inside the eye [8]. Without correction, presbyopia prevents people from reading or effectively using a smartphone.

Many corrections exist for presbyopia. Bifocals and progressive lenses are well known examples. Monovision corrections are less well known. With monovision, each eye is fitted with a lens that sharply focuses light from a different distance, providing "near vision" to one eye and "far vision" to the other. Monovision thus causes differential blur between the eyes. When users accept monovision corrections, the visual system suppresses the lower-quality image and preferentially processes the higher quality of the two images [9–11]. The consequence is an increase in effective depth of field without many of the drawbacks of other corrections (e.g., the "seam" in the visual field caused by bifocals). Unfortunately, monovision has its own drawbacks. It degrades stereoacuity [12, 13] and contrast sensitivity [14], hampering fine-scale depth discrimination and reading in low light. Monovision is also thought to cause difficulties in driving [1], and it has been implicated in an aviation accident [15]. Despite these drawbacks, many people prefer monovision corrections to other corrections, or no corrections at all [16].

Ten million people in the United States currently have monovision corrections (see STAR Methods). The number of candidates will increase in the coming years. The population is aging, and monovision is the most popular contact lens correction for presbyopia among the baby boomers [16]. A full understanding of the effects of monovision on vision is critical. However, there is no literature on how the differential blur induced by monovision impacts motion perception, which is critical for successful interaction with the environment [17].

We investigated the impact of differential blur on motion perception by measuring the Pulfrich effect, a stereo-motion phenomenon first reported nearly 100 years ago [2]. When a target oscillates horizontally in the frontoparallel plane and is viewed with unequal retinal illuminance or contrast in the two eyes [2, 18], it appears to move on an elliptical trajectory in depth (Figure 1A). The effect occurs because the image in the eye with lower retinal illuminance or contrast is processed more slowly than the image in the other eye [2, 18, 19]. The mismatch in processing speed causes a neural binocular disparity, a difference in the effective target image locations in the two retinas [20, 21]. The disparity results in the illusory motion in depth. The Pulfrich effect has been researched extensively since its first discovery [18, 19, 22–27]. In the late 1990s and early 2000s, a flurry of work debated what the effect reveals about the neural basis of stereo and motion encoding [28–31]. But it is not known

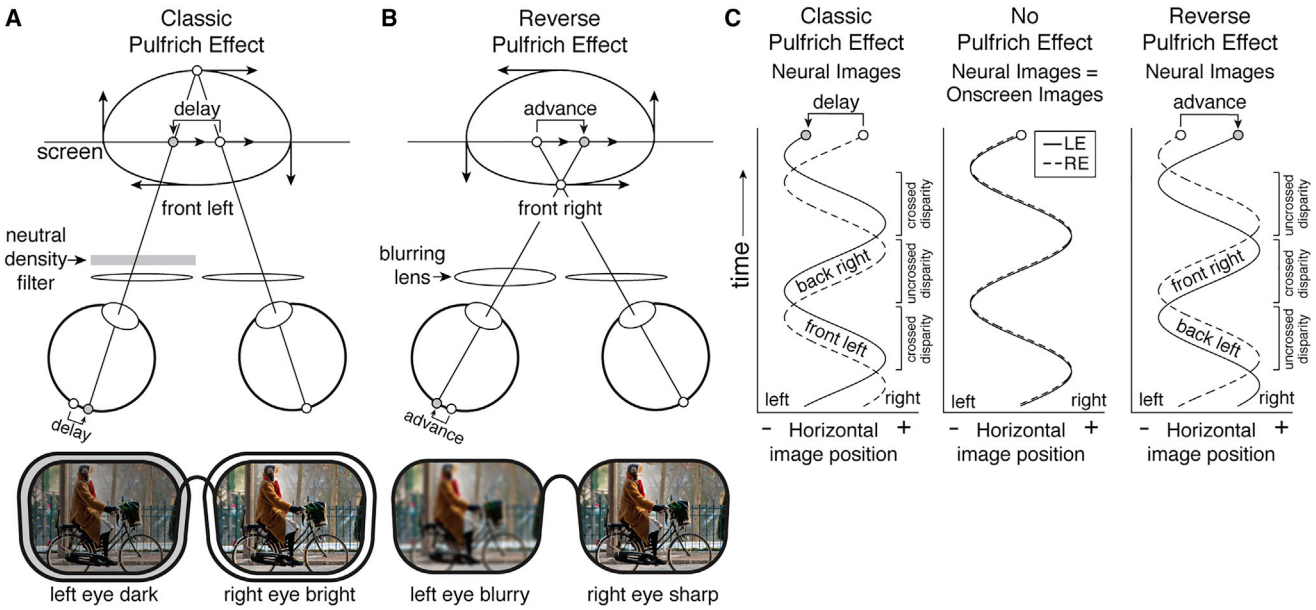

Figure 1. Classic and Reverse Pulfrich Effects

(A) Classic Pulfrich effect. A left-eye neutral density filter causes horizontally oscillating frontoparallel motion to be misperceived in depth (i.e., "front-left"; clockwise motion from above). The image in the eye with lower retinal illuminance (gray dot) is delayed relative to the other eye (white dot), causing a neural disparity.

(B) Reverse Pulfrich effect. A left-eye blurring lens causes illusory motion in depth in the other direction (i.e., "front-right"). The blurrier image (gray dot) is advanced relative to the other eye (white dot), causing a neural disparity with the opposite sign.

(C) Neural image positions across time for the classic Pulfrich effect, no Pulfrich effect, and the reverse Pulfrich effect.

whether the Pulfrich effect is caused by the optical conditions induced by monovision corrections.

Do interocular blur differences, like interocular illuminance and contrast differences, cause misperceptions of motion? More specifically, does blur slow the speed of processing and cause a Pulfrich effect? In the classic Pulfrich effect, if the left eye retinal illuminance or contrast is decreased, observers perceive "front-left" motion (i.e., clockwise motion from above; Figure 1A). However, we find that when the left eye is blurred, observers perceive "front-right" motion (Figure 1B). Thus, instead of a classic Pulfrich effect, differential blur causes a reverse Pulfrich effect.

The reverse Pulfrich effect implies an apparent paradox. Blur reduces contrast and should therefore cause the blurry image to be processed more slowly, but the reverse Pulfrich effect implies that the blurry image is processed more quickly (Figure 1C). At first, this finding appears at odds with a large body of neurophysiological and behavioral results. Low-contrast images are known to be processed more slowly in early visual cortex [4, 6, 32] and at the level of behavior [3, 5].

The paradox is resolved by recognizing two facts. First, blur reduces the contrast of high-spatial-frequency image components more than low-frequency image components [33–35]. Second, extensive neurophysiological [6, 32, 36, 37] and behavioral [3, 5] literatures indicate that high spatial frequencies are processed more slowly than low spatial frequencies, all else equal. Together, these facts suggest that the blurry image is processed more quickly than the sharp image because the high spatial frequencies in the sharp image decrease the speed at which it is processed. Thus, the reverse Pulfrich effect can be explained by known properties of the early visual system.

Psychophysical Results

To measure the reverse Pulfrich effect, we performed a one-interval two-alternative forced choice (2AFC) experiment. We used trial lenses to induce interocular differences in blur and a haploscope for dichoptic presentation of moving targets (Figure 2A). On each trial, a target oscillated from left to right (or right to left) while the observer fixated a central dot. The onscreen interocular delay of the target images was under experimenter control. If the onscreen delay is zero, onscreen disparity specifies that the target is moving in the plane of the screen. If the onscreen delay is non-zero, onscreen disparity specifies that the target is moving on an elliptical trajectory outside the plane of the screen. Observers reported whether the target was moving leftward or rightward when it appeared to be in front of the screen. Human observers made these judgments easily and reliably.

For a given difference in focus error, we measured the proportion of trials that observers reported "front right" as a function of the onscreen interocular delay. In each condition, performance was summarized with the point of subjective equality (PSE), the 50% point on the psychometric function (Figures 2B and 2C). The PSE specifies the onscreen delay required to make the target appear to move in the plane of the screen (i.e., no motion in depth).

The magnitude of the reverse Pulfrich effect increases with the difference in focus error between the eyes (Figure 2B, white circles; Figure S1). (Discrimination thresholds also increase with differences in focus error [12]; Figures 2C and S1.) Negative differences indicate conditions in which the left-eye retinal image is blurry and the right-eye retinal image

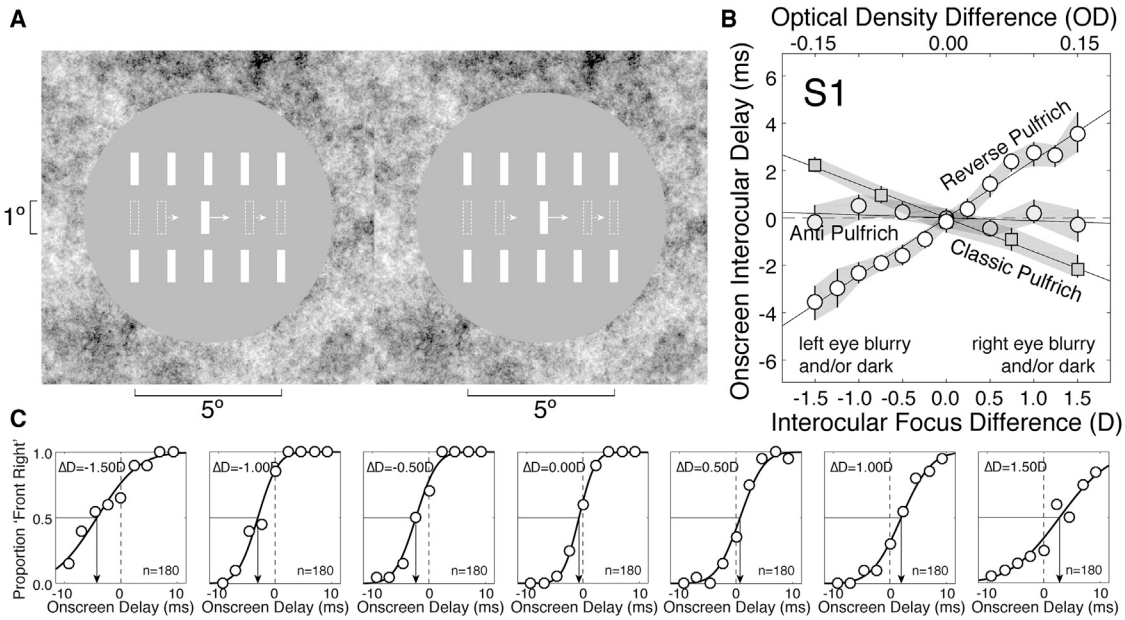

Figure 2. Reverse, Classic, and Anti-Pulfrich Conditions: Psychophysical Data

(A) Binocular stimulus. The target was a horizontally moving 0.25° × 1.0° white bar. Arrows show motion, speed, and direction, and dashed bars show bar positions during a trial; both are for illustrative purposes only and were not in the actual stimulus. Observers reported whether they saw three-dimensional (3D) target motion as front-right or front-left with respect to the screen. Fuse the two half-images to perceive the stimulus in 3D. Cross and divergent fusers will perceive the bar nearer and farther than the screen, respectively.

(B) Points of subjective equality (PSEs) for one observer, expressed as onscreen interocular delay relative to baseline. Interocular differences in focus error (bottom axis, white circles) cause the reverse Pulfrich effect. Interocular differences in retinal illuminance (top axis, gray squares) cause the classic Pulfrich effect. Appropriately tinting the blurring lens (light gray circles) can eliminate the motion illusions and act as an anti-Pulfrich correction. (In the anti-Pulfrich conditions, optical density was different for each observer and focus difference.) Shaded regions indicate bootstrapped standard errors. Best-fit regression lines are also shown.

(C) Psychometric functions for seven of the reverse Pulfrich conditions in (B). Arrows indicate raw PSEs.

See also Figure S1.

is sharp. In these conditions, the left-eye onscreen image must be delayed (i.e., negative PSE shift) for the target to be perceived as moving in the screen plane. Positive differences in focus error indicate that the left-eye retinal image is sharp and the right-eye retinal image is blurry. In these conditions, the right-eye onscreen image must be delayed (i.e., positive PSE shift). The results indicate that the blurrier image is processed faster. For the first observer, a ±1.5D difference in focus error caused an interocular difference in processing speed of ±3.7 ms (Figure 2B).

As a control, we measured the classic Pulfrich effect. Systematically reducing the retinal illuminance to one eye, while leaving the other eye unperturbed, reverses the pattern of PSE shifts (Figure 2B, gray squares; Figure S1). When the left eye's retinal illuminance is reduced, the left-eye onscreen image must be advanced in time for the target to be perceived as moving in the plane of the screen, and vice versa. Consistent with classic findings, these results indicate that the darker image is processed more slowly than the brighter image.

Why does the reverse Pulfrich effect occur? To test the hypothesis that high spatial frequencies in the sharp image slow down its processing (see above), we ran an additional experiment. In the first condition, the onscreen stimulus to one eye was high-pass filtered while the other stimulus was unperturbed. High-pass filtering sharpens the image by removing low frequencies, increases the average spatial frequency, and should decrease the processing speed relative to the original unperturbed stimulus. In the second condition, the onscreen stimulus to one eye was low-pass filtered (Figures 3A and 3B). Low-pass filtering removes high frequencies, approximates the effects of optical blur, and should increase processing speed. Results with high- and low-pass filtered stimuli should therefore resemble the classic and reverse Pulfrich effects, respectively. This prediction is confirmed by the data (Figures 3C and S2). Importantly, the interocular differences in processing speed cannot be attributed to luminance or contrast differences because the filtered stimuli were designed to have identical luminance and contrast (Figure S2). The computational rules that relate frequency content to processing speed remain to be worked out and should make a fruitful area for future study. A full understanding of these rules may facilitate the construction of stimuli that yield larger effect sizes than those reported here [37].

The performance of the first human observer is consistent across all observers and experiments (Figures 3D, S1, and S2). The interocular differences in processing speed were 1.4–3.7 ms across observers for 1.5D differences in focus error and 1.5–2.1 ms for 0.15OD differences in retinal illuminance. Similar effects are obtained with low- and high-pass filtering. These differences in processing speed may appear modest.

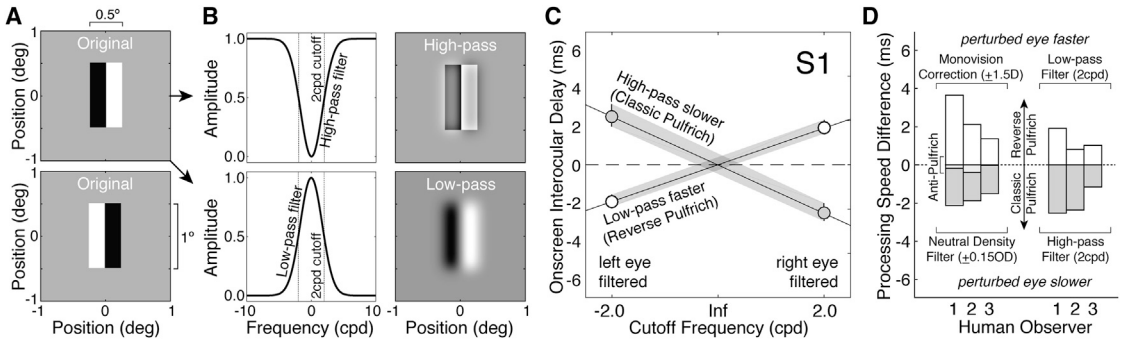

Figure 3. Spatial Frequency Filtering: Psychophysical Data

(A) Original stimuli were composed of adjacent black-white (top) or white-black (bottom) 0.25° × 1.00° bars.

(B) High-pass or low-pass filtered stimuli (shown only for black-white bar stimuli). High- and low-pass filtered stimuli were designed to have identical luminance and contrast (see Figure S2).

(C) Resulting interocular delays. High-pass filtered stimuli are processed more slowly, and low-pass filtered stimuli are processed more quickly than the original unfiltered stimulus. Negative cutoff frequencies indicate that the left eye was filtered (high or low pass). Positive cutoff frequencies indicate that the right eye was filtered.

(D) Effect sizes for each human observer in multiple conditions, obtained from the best-fit regression lines (see Figures 2B and 3C). Two manipulations resulted in reverse Pulfrich effects (white bars): blurring one eye (left) and low-pass filtering one eye (right). Two manipulations resulted in classic Pulfrich effects (gray bars): darkening one eye (left) and high-pass filtering one eye (right). A fifth manipulation—appropriately darkening the blurring lens (left, small light-gray bars)—eliminates the Pulfrich effect and acts as an anti-Pulfrich correction.

However, a difference of a few milliseconds in processing speed can lead to dramatic illusions in depth (see below).

Effect sizes vary across observers but appear correlated in each observer across conditions (Figure 3D). A larger pool of observers is necessary to confirm this trend. Future studies should measure the range and determine the origin of these inter-observer differences. Developing techniques that increase the speed of data collection will aid these efforts [38].

Motion Illusions in the Real World

Monovision corrections cause misperceptions of motion. How large will these misperceptions be in daily life? If the illusions are small, they can be safely ignored. If the illusions are large, they may have serious consequences. To predict the severity of misperceptions in real-world viewing, differences in pupil size, target speed, and viewing distance must be taken into account (see STAR Methods). The same focus error causes less blur with smaller pupils. The same interocular difference in processing speed causes larger neural disparities at faster speeds. The same disparity specifies larger depths at longer viewing distances.

Consider a target object, five meters away, moving from left to right in daylight conditions. Predicted illusion sizes with different monovision corrections strengths are shown for one observer as a function of target speed (Figure 4A). A +1.5D difference in optical power (far lens over left eye), a common monovision correction strength [1], will cause the distance of a target moving at 15 miles per hour to be overestimated by 2.8 m. This, remarkably, is the width of a narrow street lane! If the prescription is reversed (−1.5D; far lens over right eye) target distance will be underestimated by 1.3 m. Also, illusion sizes should increase with faster target speeds, stronger monovision corrections, and dimmer lighting conditions [19, 23, 24, 39] (e.g., driving at dawn, dusk, or night; see STAR Methods).

Illusions this large will not only be disturbing for the person wearing the monovision correction; they may compromise public safety. In countries where motorists drive on the right side of the road (e.g., the US), cars and cyclists in the near lane of cross traffic move from left to right. Placing the far lens in the left eye will cause distance overestimation, which may result in casual braking and increase the likelihood of traffic accidents (Figure 4B). Placing the far lens in the right eye may be advisable. Doing so should result in distance underestimation and more cautious braking, which may reduce the likelihood of collisions (Figure 4C). In countries where motorists drive on the left side of the road (e.g., the United Kingdom), the opposite practice should be considered (i.e., far lens in left eye). The current standard is to place the far lens in the dominant eye [1, 41], but this practice does not improve patient acceptance rate, patient satisfaction [41, 42], or quantitative measures of visual performance [13, 43]. The scenarios described here may invite reexamination of standard ophthalmic practice.

In the real world, many cues exist that tend to indicate the correct rather than illusory depths. The literature on cue combination [44, 45] suggests that in cue rich situations, the magnitude of the reverse Pulfrich effect may be somewhat reduced from the predictions in Figure 4A. Determining which cues are most important [46] and examining how the reverse Pulfrich effect manifests in real-world viewing conditions will be of clinical and scientific interest. These issues could be examined with virtual- or augmented-reality headsets that provide precise programmatic control of near-photorealistic graphical renderings.

Another implication of these results is that objects moving toward an observer along straight lines should appear to follow S-curve trajectories (Figure S3). These misperceptions should make it difficult to play tennis, baseball, and other ball sports requiring accurate perception of moving targets. Monovision corrections should be avoided when playing these sports.

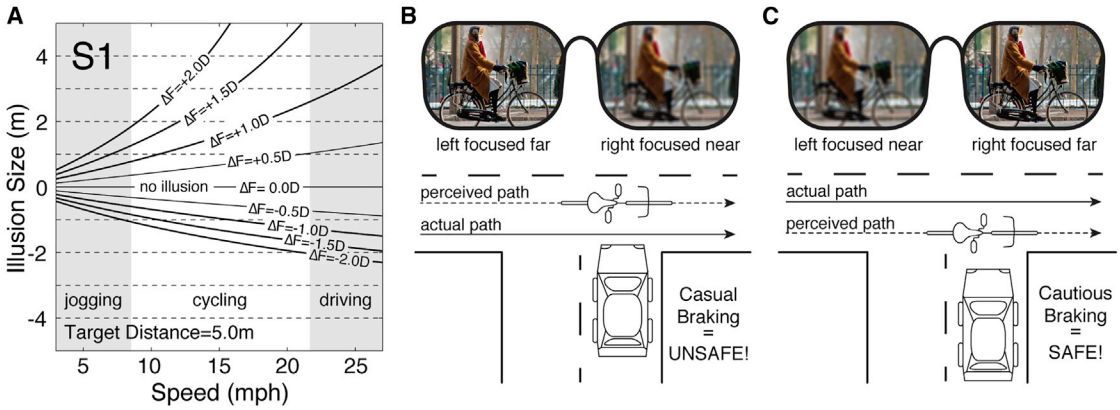

Figure 4. Monovision Corrections and Real-World Misperceptions of Depth

(A) Illusion size as a function of speed for an object moving from left to right at 5.0 m, with different monovision corrections strengths (curves). Monovision correction strengths (interocular focus difference, ΔF) typically range between 1.0D and 2.0D [1]. Shaded regions show speeds associated with jogging, cycling, and driving. Illusion sizes are predicted from stereo-geometry, assuming a pupil size (2.1mm) that is typical for daylight conditions [39] and interocular delays that were measured from observer S1 (see Figure 2B). The predictions assume that the observer can focus the target at 5.0 m in one eye [40].

(B) The distance of cross traffic moving from left to right will be overestimated when the left eye is focused far (sharp) and the right eye is focused near (blurry).

(C) The distance of left-to-right cross traffic will be underestimated when the left and right eyes are focused near and far, respectively.

See also Figure S3.

Eliminating Monovision-Induced Motion Illusions

Reconsidering prescribing practices is one approach to minimizing the consequences of monovision-induced motion illusions, but it is not the perfect solution. It would be far preferable to eliminate the illusions altogether. Because increased blur and reduced retinal illuminance have opposite effects on processing speed, it should be possible to null the two effects by tinting the blurring lens. We reran the original experiment with appropriately tinted blurring lenses for each human observer (see STAR Methods). This "anti-Pulfrich correction" eliminates the motion illusion in all human observers (Figures 2B and 3D). Of course, for a given monovision prescription, the lens forming the blurry image varies with target distance. Anti-Pulfrich monovision corrections thus cannot work at all target distances. Tinting the near lens (blurry, dark images for far targets; sharp, dark images for near targets) will eliminate the Pulfrich effect for far targets but exacerbate it for near targets. However, because many presbyopes retain some accommodation and use it to focus the distance-corrected eye [40], the range of far distances for which motion misperceptions may be eliminated can be quite large: 0.67 m to the horizon for a presbyope with 1.5D of residual accommodation. Given that accurate perception of moving targets is probably more important for tasks at far than at near distances (e.g., driving versus reading), tinting the near lens is likely to be the preferred solution. This issue, however, clearly needs further study.

Adaptation

Previous studies have shown that blur perception changes with consistent exposure to blur [47]. Do motion illusions change over time as patients adapt to monovision corrections? The literature on adaptation to the classic Pulfrich effect may provide a guide [22, 24, 48, 49]. However, in these adaptation studies, the eye with the dark image was fixed. With monovision corrections, the eye with the blurry image varies with target distance. Thus, it is unclear whether observers will adapt away motion illusions caused by differential blur. This is an important area for future study, both for basic science and for the development of successful clinical interventions.

Spatial-Frequency Binding Problem

Scientific discoveries often present new scientific opportunities. We have argued that the reverse Pulfrich effect occurs because sharp images contain more high frequencies (i.e., fine details) than blurry images and because high frequencies are processed more slowly than low frequencies. Indeed, different spatial frequencies are processed in early visual cortex with different latencies [37]. Thus, the frequency components of an image should appear to split apart when a target object moves, causing rigidly moving images to appear non-rigid. This percept is not typically experienced. To achieve a unified percept, the visual system must therefore have a mechanism for binding the different frequency components together.

Variants of the paradigm that we have used to measure the reverse Pulfrich effect have great potential for investigating the visual system's solution to the spatial-frequency binding problem. The measurements have exquisite temporal precision, often to within fractions of a millisecond (Figures 2B, 2C, 3C, and 3D). This precision should prove useful for studying this fundamentally important but understudied problem in vision and visual neuroscience.

We have reported a new version of a 100-year-old illusion: the reverse Pulfrich effect. We found that interocular differences in image blur, like those caused by monovision corrections, cause millisecond interocular differences in processing speed. For moving targets, these differences cause dramatic illusions of motion in depth. The fact that mismatches of a few milliseconds can cause substantial misperceptions highlights how exquisitely the visual system must be calibrated for accurate percepts to occur. The fact that these misperceptions are rare indicates how well the visual system is calibrated under normal circumstances.

STAR★METHODS

Detailed methods are provided in the online version of this paper and include the following:

- KEY RESOURCES TABLE
- LEAD CONTACT AND MATERIALS AVAILABILITY
- EXPERIMENTAL MODEL AND SUBJECT DETAILS
- METHOD DETAILS
  - Prevalence of monovision corrections
  - Apparatus
  - Stimuli
  - Procedure
  - Defocus and blur
  - Neutral density filters
  - Low- and high-pass spatial filtering
  - Generalizing results to the real world
  - Anti-Pulfrich monovision corrections
- QUANTIFICATION AND STATISTICAL ANALYSIS
- DATA AND CODE AVAILABILITY

SUPPLEMENTAL INFORMATION

Supplemental Information can be found online at https://doi.org/10.1016/j.cub.2019.06.070.

ACKNOWLEDGMENTS

We thank Bill Geisler, David Brainard, Josh Gold, Marty Banks, and Mike Landy for useful feedback; Larry Cormack for help constructing the haploscope; and VPixx for custom firmware to support simultaneous presentation of high-resolution images on two monitors at high frame rates. This work was supported by NIH grant R01-EY028571 from the National Eye Institute and the Office of Social and Behavioral Science to J.B., startup funds from the University of Pennsylvania to J.B., Spanish Ministry of Education grant FPU17/02760 to V.R.L., and Spanish Ministry of Science, Innovation, and Universities grants ISCIII DTS2016/00127 and FIS2017-84753-R to C.D.

AUTHOR CONTRIBUTIONS

J.B. wrote the paper. J.B. and V.R.L. collected and analyzed data. J.B., V.R.L., and C.D. conceived the project and edited the paper.

DECLARATION OF INTERESTS

A provisional patent on anti-Pulfrich monovision corrections has been filed by the University of Pennsylvania and the Institute of Optics (CSIC) with J.B., V.R.L., and C.D. as inventors.

Received: May 11, 2019
Revised: June 24, 2019
Accepted: June 24, 2019
Published: July 25, 2019

REFERENCES

1. Evans, B.J.W. (2007). Monovision: a review. Ophthalmic Physiol. Opt. *27*, 417–439.
2. Pulfrich, C. (1922). Die Stereoskopie im Dienste der isochromen und heterochromen Photometrie. Naturwissenschaften *10*, 553–564.
3. Nachmias, J. (1967). Effect of exposure duration on visual contrast sensitivity with square-wave gratings. J. Opt. Soc. Am. *57*, 421–427.
4. Shapley, R.M., and Victor, J.D. (1978). The effect of contrast on the transfer properties of cat retinal ganglion cells. J. Physiol. *285*, 275–298.
5. Levi, D.M., Harwerth, R.S., and Manny, R.E. (1979). Suprathreshold spatial frequency detection and binocular interaction in strabismic and anisometropic amblyopia. Invest. Ophthalmol. Vis. Sci. *18*, 714–725.
6. Albrecht, D.G. (1995). Visual cortex neurons in monkey and cat: effect of contrast on the spatial and temporal phase transfer functions. Vis. Neurosci. *12*, 1191–1210.
7. Fricke, T.R., Tahhan, N., Resnikoff, S., Papas, E., Burnett, A., Ho, S.M., Naduvilath, T., and Naidoo, K.S. (2018). Global prevalence of presbyopia and vision impairment from uncorrected presbyopia: systematic review, meta-analysis, and modelling. Ophthalmology *125*, 1492–1499.
8. Charman, W.N. (2008). The eye in focus: accommodation and presbyopia. Clin. Exp. Optom. *91*, 207–225.
9. Westendorf, D.H., Blake, R., Sloane, M., and Chambers, D. (1982). Binocular summation occurs during interocular suppression. J. Exp. Psychol. Hum. Percept. Perform. *8*, 81–90.
10. Schor, C., Landsman, L., and Erickson, P. (1987). Ocular dominance and the interocular suppression of blur in monovision. Am. J. Optom. Physiol. Opt. *64*, 723–730.
11. Zheleznyak, L., Sabesan, R., Oh, J.-S., MacRae, S., and Yoon, G. (2013). Modified monovision with spherical aberration to improve presbyopic through-focus visual performance. Invest. Ophthalmol. Vis. Sci. *54*, 3157–3165.
12. Westheimer, G., and McKee, S.P. (1980). Stereoscopic acuity with defocused and spatially filtered retinal images. J. Opt. Soc. Am. A *70*, 772–778.
13. McGill, E., and Erickson, P. (1988). Stereopsis in presbyopes wearing monovision and simultaneous vision bifocal contact lenses. Am. J. Optom. Physiol. Opt. *65*, 619–626.
14. Pardhan, S., and Gilchrist, J. (1990). The effect of monocular defocus on binocular contrast sensitivity. Ophthalmic Physiol. Opt. *10*, 33–36.
15. Nakagawara, V.B., and Véronneau, S.J. (2000). Monovision contact lens use in the aviation environment: a report of a contact lens-related aircraft accident. Optometry *71*, 390–395.
16. Bennett, E.S. (2008). Contact lens correction of presbyopia. Clin. Exp. Optom. *91*, 265–278.
17. Burge, J., and Geisler, W.S. (2015). Optimal speed estimation in natural image movies predicts human performance. Nat. Commun. *6*, 7900.
18. Reynaud, A., and Hess, R.F. (2017). Interocular contrast difference drives illusory 3D percept. Sci. Rep. *7*, 5587.
19. Lit, A. (1949). The magnitude of the Pulfrich stereophenomenon as a function of binocular differences of intensity at various levels of illumination. Am. J. Psychol. *62*, 159–181.
20. Wheatstone, C. (1838). On some remarkable, and hitherto unobserved, phenomena of binocular vision. Philos. Trans. R. Soc. Lond. *128*, 371–394.
21. Burge, J., and Geisler, W.S. (2014). Optimal disparity estimation in natural stereo images. J. Vis. *14*, 1.
22. Standing, L.G., Dodwell, P.C., and Lang, D. (1968). Dark adaptation and the pulfrich effect. Percept. Psychophys. *4*, 118–120.
23. Wilson, J.A., and Anstis, S.M. (1969). Visual delay as a function of luminance. Am. J. Psychol. *82*, 350–358.
24. Rogers, B.J., and Anstis, S.M. (1972). Intensity versus adaptation and the Pulfrich stereophenomenon. Vision Res. *12*, 909–928.
25. Morgan, M.J., and Thompson, P. (1975). Apparent motion and the Pulfrich effect. Perception *4*, 3–18.
26. Carney, T., Paradiso, M.A., and Freeman, R.D. (1989). A physiological correlate of the Pulfrich effect in cortical neurons of the cat. Vision Res. *29*, 155–165.
27. Lages, M., Mamassian, P., and Graf, E.W. (2003). Spatial and temporal tuning of motion in depth. Vision Res. *43*, 2861–2873.
28. Qian, N., and Andersen, R.A. (1997). A physiological model for motion-stereo integration and a unified explanation of Pulfrich-like phenomena. Vision Res. *37*, 1683–1698.

29. Read, J.C.A., and Cumming, B.G. (2005). All Pulfrich-like illusions can be explained without joint encoding of motion and disparity. J. Vis. *5*, 901–927.
30. Read, J.C.A., and Cumming, B.G. (2005). The stroboscopic Pulfrich effect is not evidence for the joint encoding of motion and depth. J. Vis. *5*, 417–434.
31. Qian N, Freeman RD. Pulfrich phenomena are coded effectively by a joint motion-disparity process. Journal of Vision 9, 24.
32. Bair, W., and Movshon, J.A. (2004). Adaptive temporal integration of motion in direction-selective neurons in macaque visual cortex. J. Neurosci. *24*, 7305–7323.
33. Campbell, F.W., and Green, D.G. (1965). Optical and retinal factors affecting visual resolution. J. Physiol. *181*, 576–593.
34. Navarro, R., Artal, P., and Williams, D.R. (1993). Modulation transfer of the human eye as a function of retinal eccentricity. J. Opt. Soc. Am. A *10*, 201–212.
35. Burge, J., and Geisler, W.S. (2011). Optimal defocus estimation in individual natural images. Proc. Natl. Acad. Sci. USA *108*, 16849–16854.
36. Breitmeyer, B.G., and Ganz, L. (1977). Temporal studies with flashed gratings: inferences about human transient and sustained channels. Vision Res. *17*, 861–865.
37. Vassilev, A., Mihaylova, M., and Bonnet, C. (2002). On the delay in processing high spatial frequency visual information: reaction time and VEP latency study of the effect of local intensity of stimulation. Vision Res. *42*, 851–864.
38. Bonnen, K., Burge, J., Yates, J., Pillow, J., and Cormack, L.K. (2015). Continuous psychophysics: target-tracking to measure visual sensitivity. J. Vis. *15*, 14.
39. Stockman, A., and Sharpe, L.T. (2006). Into the twilight zone: the complexities of mesopic vision and luminous efficiency. Ophthalmic Physiol. Opt. *26*, 225–239.
40. Almutairi, M.S., Altoaimi, B.H., and Bradley, A. (2018). Accommodation in early presbyopes fit with bilateral or unilateral near add. Optom. Vis. Sci. *95*, 43–52.
41. Wolffsohn, J.S., and Davies, L.N. (2019). Presbyopia: effectiveness of correction strategies. Prog. Retin. Eye Res. *68*, 124–143.
42. Schor, C., Carson, M., Peterson, G., Suzuki, J., and Erickson, P. (1989). Effects of interocular blur suppression ability on monovision task performance. J. Am. Optom. Assoc. *60*, 188–192.
43. Erickson, P., and Schor, C. (1990). Visual function with presbyopic contact lens correction. Optom. Vis. Sci. *67*, 22–28.
44. Landy, M.S., Maloney, L.T., Johnston, E.B., and Young, M. (1995). Measurement and modeling of depth cue combination: in defense of weak fusion. Vision Res. *35*, 389–412.
45. Ernst, M.O., and Banks, M.S. (2002). Humans integrate visual and haptic information in a statistically optimal fashion. Nature *415*, 429–433.
46. Burge, J., and Jaini, P. (2017). Accuracy maximization analysis for sensory-perceptual tasks: computational improvements, filter robustness, and coding advantages for scaled additive noise. PLoS Comput. Biol. *13*, e1005281.
47. Radhakrishnan, A., Dorronsoro, C., Sawides, L., Webster, M.A., and Marcos, S. (2015). A cyclopean neural mechanism compensating for optical differences between the eyes. Curr. Biol. *25*, R188–R189.
48. Wolpert, D.M., Miall, R.C., Cumming, B., and Boniface, S.J. (1993). Retinal adaptation of visual processing time delays. Vision Res. *33*, 1421–1430.
49. Plainis, S., Petratou, D., Giannakopoulou, T., Radhakrishnan, H., Pallikaris, I.G., and Charman, W.N. (2013). Interocular differences in visual latency induced by reduced-aperture monovision. Ophthalmic Physiol. Opt. *33*, 123–129.
50. Brainard, D.H. (1997). The psychophysics toolbox. Spat. Vis. *10*, 433–436.
51. United States Census Bureau. U.S. and world population clock, https://www.census.gov/popclock.
52. Cope, J.R., Collier, S.A., Rao, M.M., Chalmers, R., Mitchell, G.L., Richdale, K., Wagner, H., Kinoshita, B.T., Lam, D.Y., Sorbara, L., et al. (2015). Contact lens wearer demographics and risk behaviors for contact lens-related eye infections–United States, 2014. MMWR Morb. Mortal. Wkly. Rep. *64*, 865–870.
53. Morgan, P.B., Woods, C.A., Tranoudis, I.O., Efron, N., Jones, L., Aighamdi, W., Nair, V., Merchan, N.L., Teufl, I./M., Grupcheva, C.N., et al. (2019). International contact lens prescribing in 2018. Contact Lens Spectr. *34*, 26–32.
54. National Eye Institute. Cataracts defined tables, https://nei.nih.gov/eyedata/cataract/tables.
55. Ingenito, K. (2015). Premium cataract options gain ground. Ophthalmol. Manage. *19*, 42–43.

STAR★METHODS

KEY RESOURCES TABLE

REAGENT or RESOURCE	SOURCE	IDENTIFIER
Deposited Data		
Raw data	This paper	http://doi.org/10.5281/zenodo.3245222
Software and Algorithms		
MATLAB 2017b	Mathworks Inc., USA	http://mathworks.com/
Psychophysics Toolbox	[50]	http://psychtoolbox.org
Data analysis code	This paper	http://doi.org/10.5281/zenodo.3245222

LEAD CONTACT AND MATERIALS AVAILABILITY

Further information and requests for resources should be directed to and will be fulfilled by the Lead Contact, Johannes Burge (jburge@psych.upenn.edu). This study did not generate new unique reagents.

EXPERIMENTAL MODEL AND SUBJECT DETAILS

Three human observers ran in the experiment; two were authors. All human observers had normal or corrected to normal visual acuity (20/20), a history of isometropia, and normal stereoacuity as confirmed by the Titmus Stereo Test. The observers were aged 24, 29, 40 years old and had refractive errors of −4.75D, 0.00D, and 0.00D diopters, respectively, at the time of the measurements. Two observers were males; the other was female. The experimental protocols were approved by the Institutional Review Board at the University of Pennsylvania and were in compliance with the Declaration of Helsinki.

METHOD DETAILS

Prevalence of monovision corrections

There are approximately 123 million presbyopes in the USA [51]. Approximately 12.9 million of these presbyopes wear contact lenses, and 4.5 million (35%) of these contact lens wearers have monovision corrections [52, 53]. Approximately 30 million presbyopes have had surgery to implant intraocular lenses [54], and approximately 5.1 million (17%) of these surgical patients have received monovision corrections [55]. Together, this results in approximately 9.6 million presbyopes with monovision corrections in the USA.

Apparatus

Stimuli were displayed on a custom-built four-mirror haploscope. Left- and right-eye images were presented on two identical VPixx VIEWPixx LED monitors. Monitors were calibrated (i.e., the gamma functions were linearized) using custom software routines. The monitors had a size of 52.2x29.1cm, spatial resolution of 1920x1080 pixels, a native refresh rate of 120Hz, and a maximum luminance of 105.9cd/m^2. The maximum luminance after light loss due to mirror reflections was 93.9cd/m^2. The monitors were daisy-chained together and controlled by the same AMD FirePro D500 graphics card with 3GB GDDR5 VRAM to ensure that the left and right eye images were presented synchronously. Custom firmware was written so that each monitor was driven by a single color channel; the red channel drove the left monitor and the green channel drove the right monitor. The single-channel drive to each monitor was then split to all three channels to enable gray scale presentation. Simultaneous measurements with two optical fibers connected to an oscilloscope confirmed that the left and right eye monitor refreshes occurred within ~5 microseconds of one another.

Human observers viewed the monitors through mirror cubes with 2.5cm circular openings positioned one inter-ocular distance apart. Heads were stabilized with a chin and forehead rest. The haploscope mirrors were adjusted such that the vergence distance matched the distance of the monitors. The light path from monitor to eye was 100cm, as confirmed both by a laser ruler measurement and by a visual comparison with a real target at 100cm. At this distance, each pixel subtended 1.09arcmin. Stimulus presentation was controlled via the Psychophysics Toolbox-3 [50]. Anti-aliasing enabled sub-pixel resolution permitting accurate presentations of disparities as small as 15-20arcsec.

Stimuli

The target stimulus was a binocularly presented, horizontally moving, white vertical bar (Figure 2A). The target bar subtended 0.25° × 1.00° of visual angle. In each eye, the image of the bar moved left and right with a sinusoidal profile. An interocular phase shift between the left- and right-eye images introduced a spatial disparity between the left- and right-eye bars. The left- and right-eye onscreen bar positions were given by

$$x_L(t) = E\cos(2\pi\omega t + \phi_0 + \phi) \quad \text{(Equation 1a)}$$

$$x_R(t) = E\cos(2\pi\omega t + \phi_0) \quad \text{(Equation 1b)}$$

where x_L and x_R are the left and right eye x-positions in degrees of visual angle, E is the movement amplitude in degrees of visual angle, ω is the temporal frequency, ϕ_0 is the starting phase which in our experiment determines whether the target starts on the left or the right side of the display, t is time, and ϕ is the phase shift between the images.

The interocular temporal shift (i.e., delay or advance) in seconds associated with a particular phase shift is

$$\Delta t = \phi/(2\pi\omega) \quad \text{(Equation 2)}$$

Negative values indicate the left eye onscreen image is delayed relative to the right; positive values indicate the left eye onscreen image is advanced relative to the right.

When the interocular temporal shift equals zero, the virtual bar moves in the frontoparallel plane at the distance of the monitors. When the temporal shift is non-zero, a spatial binocular disparity results, and the virtual bar follows a near-elliptical trajectory of motion in depth. The binocular disparity in radians of visual angle as a function of time is given by

$$\delta(t) = x_R(t) - x_L(t) = 2E\sin\left(\frac{\phi}{2}\right)\sin\left(2\pi\omega t + \phi_0 + \frac{\phi}{2}\right) \quad \text{(Equation 3)}$$

Here, negative disparities are crossed and positive disparities are uncrossed, indicating that the target is nearer and farther than the screen distance, respectively. The disparity takes on its maximum magnitude when the perceived stimulus is directly in front of the observer and the lateral movement is at its maximum speed. When the stimulus is moving to the right, the maximum disparity in visual angle is given by $\delta_{max} = 2E\sin(\phi/2)$.

In our experiment, the movement amplitude was 2.5° of visual angle (i.e., 5.0° total change in visual angle in each direction), the temporal frequency was 1 cycle/s, and the starting phase ϕ_0 was randomly chosen to be either 0 or π. Restricting the starting phase to these two values forced the stimuli to start either 2.5° to the right or 2.5° to the left of center on each trial. The onscreen interocular phase shift ranged between ± 216 arcmin at maximum, corresponding to interocular delays of ± 10.0ms. The range and particular values were adjusted to the sensitivity of each human observer.

Two sets of five vertical 0.25° × 1.00° bars in a "picket fence" arrangement flanked the region of the screen traversed by the target bar. The picket fences were defined by disparity to be at the screen distance, and served as a stereoscopic reference for the observer. A 1/f noise texture, also defined by disparity to be at the screen distance, covered the periphery of the display to aid binocular fusion. A small fixation dot marked the center of the screen.

Procedure

The observer's task was to report whether the target bar was moving leftward or rightward when it appeared to be nearer than the screen on its virtual trajectory in depth. Observers fixated the fixation dot throughout each trial. Using a one-interval two-alternative forced choice procedure, nine-level psychometric functions were collected in each condition using the method of constant stimuli. Each function was fit with a cumulative Gaussian using maximum likelihood methods. The 50% point on the psychometric function—the point of subjective equality (PSE)—indicates the onscreen interocular delay needed to null the interocular difference in processing speed. The pattern of PSEs across conditions was fit via linear regression, yielding a slope and y-intercept. Average y-intercepts were nearly zero for each observer: 0.06ms, −0.06ms, and 0.01ms, respectively. To emphasize the differences in slope (i.e., the changes in processing speed in the slope) induced by interocular perturbations, we zeroed the y-intercepts when plotting the PSE data. Observers responded to 180 trials per condition in counter-balanced blocks of 90 trials each.

Defocus and blur

The interocular focus difference is the magnitude of the defocus in the right eye minus the magnitude of the defocus in the left eye

$$\Delta F = |\Delta D_R| - |\Delta D_L| \quad \text{(Equation 4)}$$

where $\Delta D = D_{focus} - D_{target}$ is the defocus, the difference between the dioptric distances of the focus and target points. To manipulate the amount of defocus blur in each eye, we positioned trial lenses ~12mm from each eye, centered on each optical axis, between each eye and the front of the mirror cubes of the haploscope.

Human observers ran in thirteen conditions defined by interocular focus difference. (One observer, S2, ran in only seven). Each eye was myopically defocused from 0.00D to 1.50D in 0.25D steps while the other eye was kept sharp. The first six conditions defocused the left eye (0.25D to 1.50D in 0.25D steps) while leaving the right eye sharp (ΔF<0.0D). In the seventh condition, both eyes were sharp (ΔF = 0.0D). The final six conditions defocused the right eye (0.25D to 1.50D in 0.25D steps) while leaving the left eye sharp (ΔF>0.0D).

In the condition in which both eyes were sharply focused, the optical distances of the left- and right-eye monitors were set to optical infinity with +1.00D trial lenses. All human observers indicated that they could sharply focus the monitor when they fully relaxed the accommodative power of their eyes. Because each trial lens absorbs a small fraction of the incident light, having a trial lens in front of

each eye in all conditions ensures that retinal illuminance is matched in both eyes in all conditions. To induce interocular differences in focus error, we placed a stronger positive lens (i.e., +1.25D, +1.50D, +1.75D, +2.00D) in front of one eye. This procedure puts one eye's monitor beyond optical infinity, thus introducing myopic focus errors that cannot be cleared by accommodation. Before each run, the observer viewed a test target to confirm that he/she could clearly focus a target at optical infinity in the 0.0D baseline condition. Undercorrected hyperopia or overcorrected myopia could place the far point of each eye beyond optical infinity, frustrating our attempts to control the optical conditions. To protect against this possibility, before running each observer, we estimated the far points of the eyes with standard optometric techniques. Then, if necessary, we adjusted the trial lens power so that the monitors were positioned at the desired optical distance.

Another potential concern is that the eyes could accommodate independently to clear the blur in each eye. However, there are several reasons to think that differential blur was successfully induced. First, positioning the optical distance of one monitor beyond optical infinity (see above) minimizes the possibility that differential optical power could be compensated by differential accommodation. Second, accommodation in the two eyes tends to be strongly coupled, especially for targets straight ahead [8, 40]. Third, discrimination thresholds $(d' = 1.0)$ increase systematically with interocular difference in focus error, which is consistent with the literature showing that differential blur deteriorates stereoacuity [12] (Figures 2C and S1).

Neutral density filters

To induce interocular differences in retinal illuminance we placed 'virtual' neutral density filters in front of the eyes. To do so, we converted optical density to transmittance, the proportion of incident light that is passed through the filter, using the standard expression $T = 10^{-OD}$ where T is transmittance and OD is optical density. Then, we reduced the luminance of one eye's monitor by a scale factor equal to the transmittance. In all observers, performance with real and equivalent virtual neutral density filters is essentially identical, suggesting that the virtual filters were implemented accurately (Figure S4).

The interocular difference in optical density $\Delta O = OD_R - OD_L$ is the difference between the optical density of filters placed over the right and left eyes. Human observers ran in five conditions with virtual neutral density filters, with equally spaced interocular differences in optical density between −0.15 and 0.15. Two conditions introduced a filter in front of the left eye (ΔO<0.00). In one condition, both eyes were unfiltered (ΔO = 0.00). And two other conditions introduced a filter in front of the right eye (ΔO>0.00).

Low- and high-pass spatial filtering

To test the hypothesis that the reverse Pulfrich effect is caused by differences in the processing speed of different spatial frequencies, we filtered the onscreen stimulus of one eye with two different frequency filters. The low-pass filter was Gaussian-shaped

$$k_{low} = \exp\left[-0.5(f/\sigma_f)^2 \right] \quad \text{(Equation 5)}$$

with a standard deviation $\sigma_f = f_0/\sqrt{\ln 4}$ set by the cutoff frequency f_0 so that the filter reached half-height at f_0 (i.e., 2cpd in the current experiments; see Figure 3). The high-pass filter complemented the low-pass filter and was given by

$$k_{high} = 1 - k_{low} \quad \text{(Equation 6)}$$

After high-pass filtering, the mean luminance was added back in so that the high-pass and low-pass filtered stimuli had the same mean luminance.

To isolate the impact of spatial frequency content on processing speed, we modified the onscreen stimulus from the main experiment. Rather than the 0.25° × 1.00° white bar, the onscreen stimulus was changed to a 0.50° × 1.00° stimulus that was composed of adjacent 0.25° × 1.0° black and white (or white and black) bars (Figure 3A). This modification ensured that the low- and high-pass filtered stimuli had identical luminance and identical contrast (see Figure S2). Each human observer collected 180 trials in each of eight conditions—low- versus high-pass filtering, left- versus right-eye filtered, black-white versus white-black stimulus types—collected in counter-balanced order. Black-white versus white-black stimulus types had little impact so results were collapsed across stimulus type.

Generalizing results to the real world

To predict the motion misperceptions that monovision will cause in the real world, it is important to account for the differences in viewing conditions that may impact illusion sizes. Although the experimental conditions were chosen based on differences in focus error, the reverse Pulfrich effect is more directly mediated by differences in image blur. The amount of retinal image blur in each eye depends both on the focus error and on the pupil diameter. Thus, it is important to account for changes in pupil diameter that will be caused by luminance differences between the lab and the viewing conditions of interest.

The blur circle diameter in radians of visual angle is given by

$$\theta_b = A|\Delta D| \quad \text{(Equation 7)}$$

where θ_b is the diameter of the blur circle in radians of visual angle and A is the pupil aperture (diameter) in meters. In our experiments, we assumed a pupil diameter of 2.5mm, corresponding to the luminance in the experiment [39]. Under the geometrical optics approximation, the absolute value of the defocus $|\Delta D|$ in the blurry eye equals the absolute value of the interocular focus difference $|\Delta F|$ because one eye was always sharply focused (i.e., $\min(|\Delta D_L|, |\Delta D_R|) = 0.0D$) in our experiments.

The interocular delay in seconds is linearly related to each level of blur by

$$\Delta t = \alpha_{\Delta F}\frac{\theta_b}{A_{exp}} + \beta_{\Delta F} \quad \text{(Equation 8)}$$

where $\alpha_{\Delta F}$ and $\beta_{\Delta F}$ are the slope and y-intercept of the best-fit line to the data in Figure 2B, and A_{exp} is the pupil diameter of the observer in meters during the experiment. The constant (i.e., y-intercept) can be dropped assuming it reflects response bias and not sensory-perceptual bias.

For a target moving at a given velocity in meters per second, a particular interocular difference in processing speed will yield an effective interocular spatial offset (i.e., position difference)

$$\Delta x = v\Delta t \quad \text{(Equation 9)}$$

The illusory distance of the target, predicted by stereo-geometry, is given by

$$\widehat{d} = \frac{I}{(I + \Delta x)}d \quad \text{(Equation 10)}$$

where I is the inter-pupillary distance and d is the actual distance of the target. Combining Equations 7–10 yields a single expression for the illusory distance

$$\widehat{d} = \left(\frac{I}{I + v|\Delta F|R\alpha_{\Delta F}}\right)d \quad \text{(Equation 11)}$$

where $R = A/A_{exp}$ is the ratio between the pupil diameters in the viewing condition of interest and in the lab when the psychophysical data was collected. Finally, taking the difference between the illusory and actual target distances $\widehat{d} - d$ yields the illusion size (see Figure 4A).

The expression for the illusory distance can also be derived by first computing the neural binocular disparity caused by the delay-induced position difference, and then converting the disparity into an estimate of depth. The binocular disparity in radians of visual angle is given by

$$\delta = \frac{\Delta x}{d} \quad \text{(Equation 12)}$$

The relationship between illusory distance, binocular disparity, and actual distance is given by

$$\widehat{d} = \frac{I}{(I + d\delta)}d \quad \text{(Equation 13)}$$

Plugging Equation 12 into Equation 13 yields Equation 10. Thus, both methods of computing the illusory distance are equivalent.

Anti-Pulfrich monovision corrections

Reducing the image quality of one eye with blur increases the processing speed relative to the other eye and causes the reverse Pulfrich effect. Reducing the retinal illuminance of one eye reduces the processing speed relative to the other eye and causes the classic Pulfrich effect. Thus, in principle, it should be possible to null the two effects by reducing the retinal illuminance of the blurry eye. The interocular delay in seconds is linearly related to each interocular difference in optical density ΔO by

$$\Delta t = \alpha_{\Delta O}(\Delta O) + \beta_{\Delta O} \quad \text{(Equation 14)}$$

The optical density that should null the interocular delay of a given interocular focus difference is given by

$$\Delta O_0 = -\frac{\alpha_{\Delta F}}{\alpha_{\Delta O}}\Delta F \quad \text{(Equation 15)}$$

the interocular difference in focus error scaled by the ratio of the slopes of the best-fit regression lines to the reverse and classic Pulfrich datasets. The optical density predicted by the two regression slopes eliminates the Pulfrich effect (Figures 2B and 3D).

QUANTIFICATION AND STATISTICAL ANALYSIS

All experiments were performed in MATLAB 2017b using Psychtoolbox (version 3.0.12) [50]. All analyses were performed in MATLAB 2017b. Psychophysical data are presented for each individual human observer. Cumulative Gaussian fits of the psychometric functions were in good agreement with the raw data. Bootstrapped standard errors are reported on all data points unless otherwise noted.

DATA AND CODE AVAILABILITY

Data and analysis code are available at http://doi.org/10.5281/zenodo.3245222. Any questions should be directed to the Lead Contact (jburge@psych.upenn.edu).

Current Biology, Volume *29*

Supplemental Information

Monovision and the Misperception of Motion

Johannes Burge, Victor Rodriguez-Lopez, and Carlos Dorronsoro

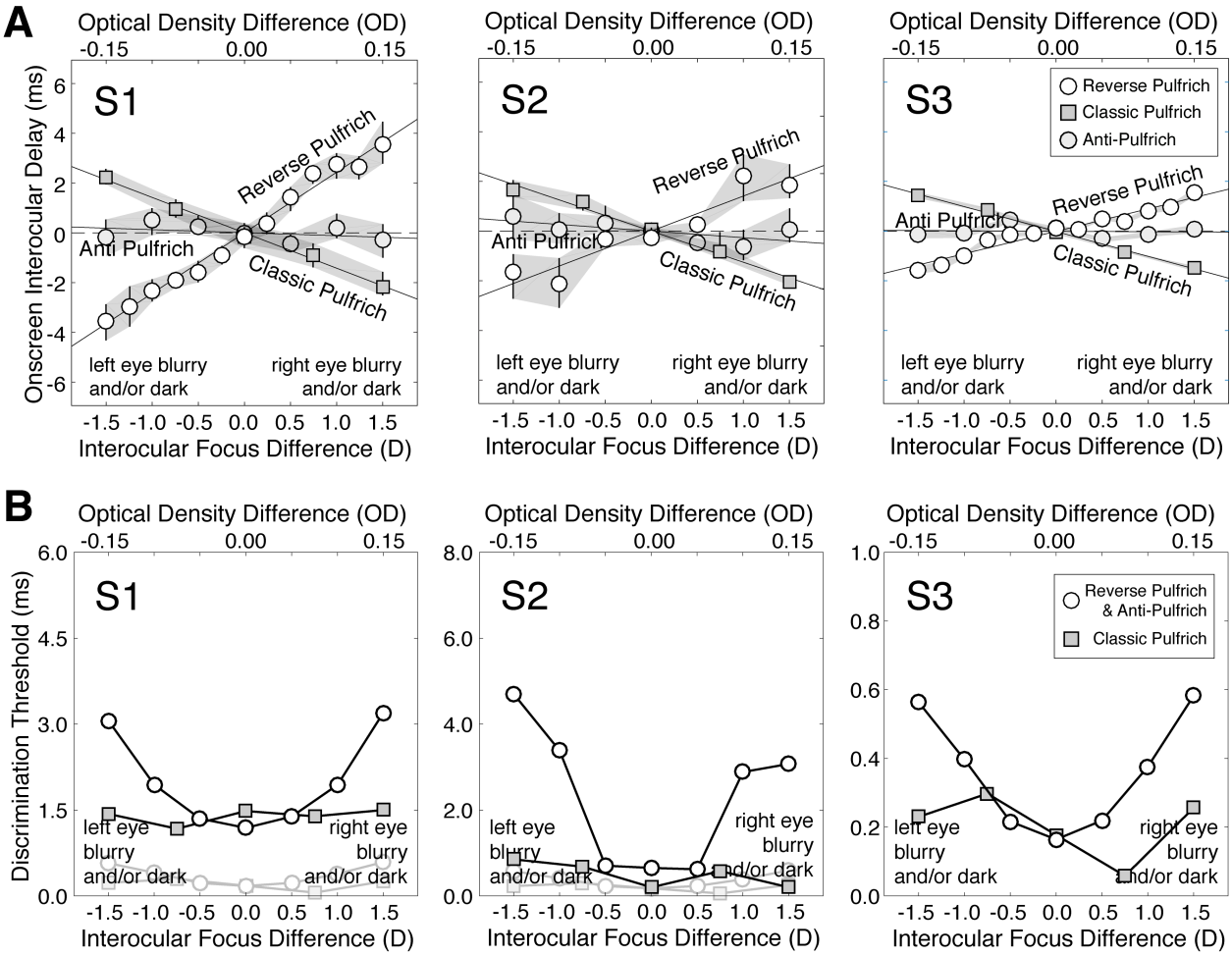

Figure S1. Reverse, classic, and anti-Pulfrich conditions: Interocular delays and discrimination thresholds. Related to Figure 2. **A** Reverse, classic, and anti-Pulfrich effects. Interocular differences in focus error cause the reverse Pulfrich effect; the blurrier image is processed more quickly. Interocular differences in retinal illuminance cause the classic Pulfrich effect; the darker image is processed more slowly. In the anti-Pulfrich condition, the blurry image is darkened to eliminate interocular delay (see Methods). **B** Discrimination thresholds. Thresholds for each observer ($d' = 1.0$) in the reverse Pulfrich conditions (interocular focus differences) and the anti-Pulfrich conditions (interocular focus differences plus retinal illuminance differences) were similar and were thus averaged together (white circles). In each human observer, discrimination thresholds increased systematically with differences in interocular blur, consistent with the classic literature on how blur differences deteriorate stereoacuity[S1]. These threshold functions thus provide evidence that the desired optical conditions were achieved. To reduce clutter, bootstrapped 95% confidence intervals are not plotted. In all cases but one, the confidence interval is smaller than the data point. Discrimination threshold in the classic Pulfrich conditions (i.e. interocular retinal illuminance differences only) are also shown (gray squares). Differences in retinal illuminance up to $\pm$0.15OD had no systematic effect on thresholds. (Note: the y-axis has a different scale for each observer to emphasize the similarities in the threshold patterns. To give a sense of scale, the classic Pulfrich data from observer S3, the most sensitive observer, is re-plotted in the subplots for observers S1 and S2; faint circles and squares.)

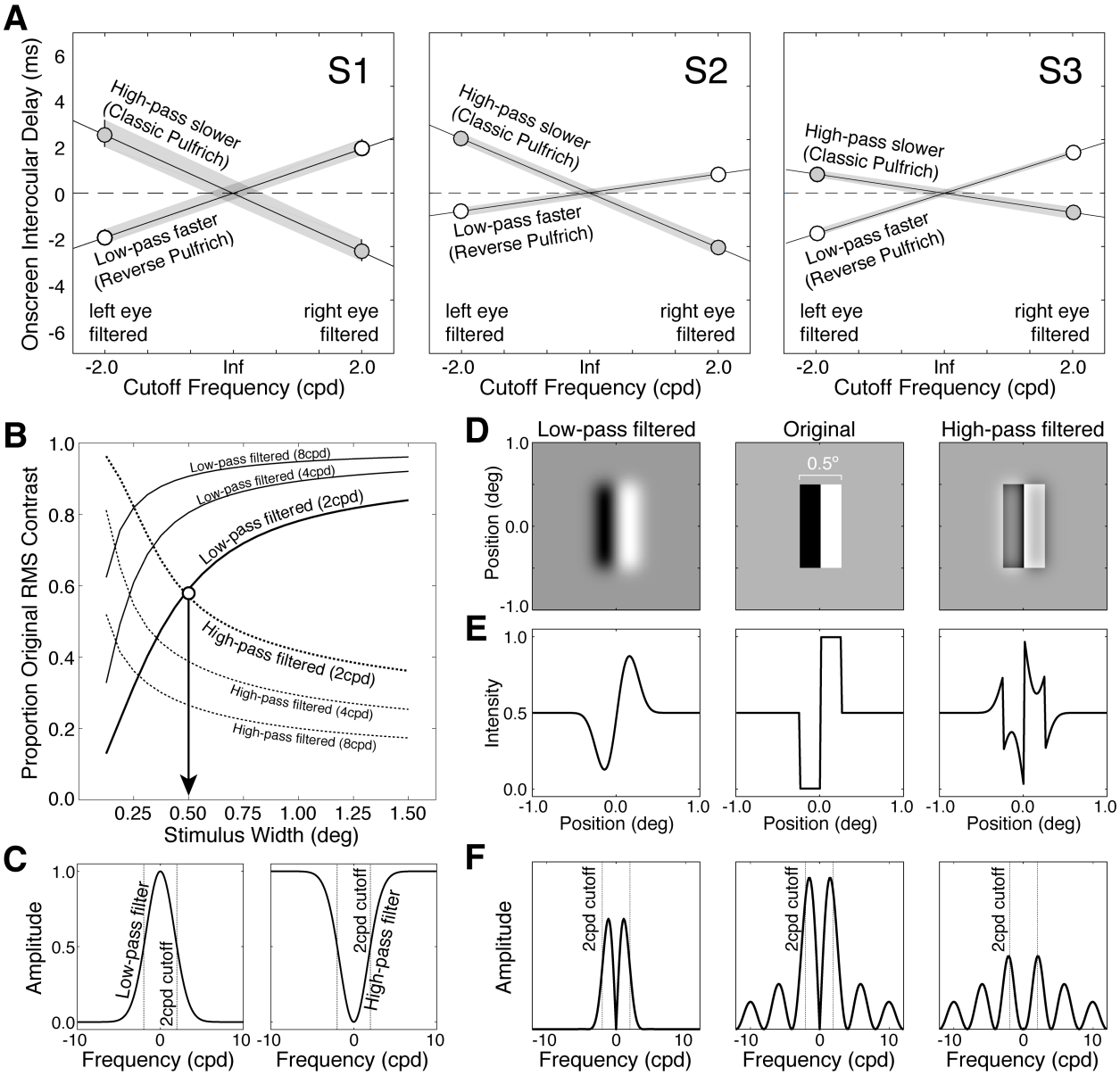

Figure S2. Spatial frequency filtered stimuli: Interocular delays and stimulus construction. Related to Figure 3. A Interocular delays with high- and low-pass filtered stimuli for each human observer. The onscreen image for one eye was filtered and the image for the other eye was left unperturbed. High-pass filtered images were processed slower than the unperturbed images, similar to how reduced retinal illuminances induces the classic Pulfrich effect. Low-pass filtered images were processed faster than unperturbed images, similar to how optical blur induces the reverse Pulfrich effect. **B** Proportion of original stimulus contrast after low-pass filtering vs. high-pass filtering (solid vs. dashed curves, respectively) as a function of total black-white (or white-black) bar width. The white circle and arrow indicate the stimulus width (0.5º) that equates the root-mean-squared (RMS) contrast of the stimulus after low- and high-pass filtering. Because low-pass and high-pass filtered images had identical luminance and contrast, the differential effects in A cannot be attributed to luminance or contrast. **C** Low-pass and high-pass filters with a 2cpd cutoff frequency. **D** Low-pass filtered stimulus, original stimulus, and high-pass filtered stimulus with matched luminance and contrast. **E** Horizontal intensity profiles of the stimuli in D. **F** Amplitude spectra of the horizontal intensity profiles in E. Note how, for each stimulus type, the peak of the lowest frequency lobe shifts relative to the cutoff frequency of the filters.

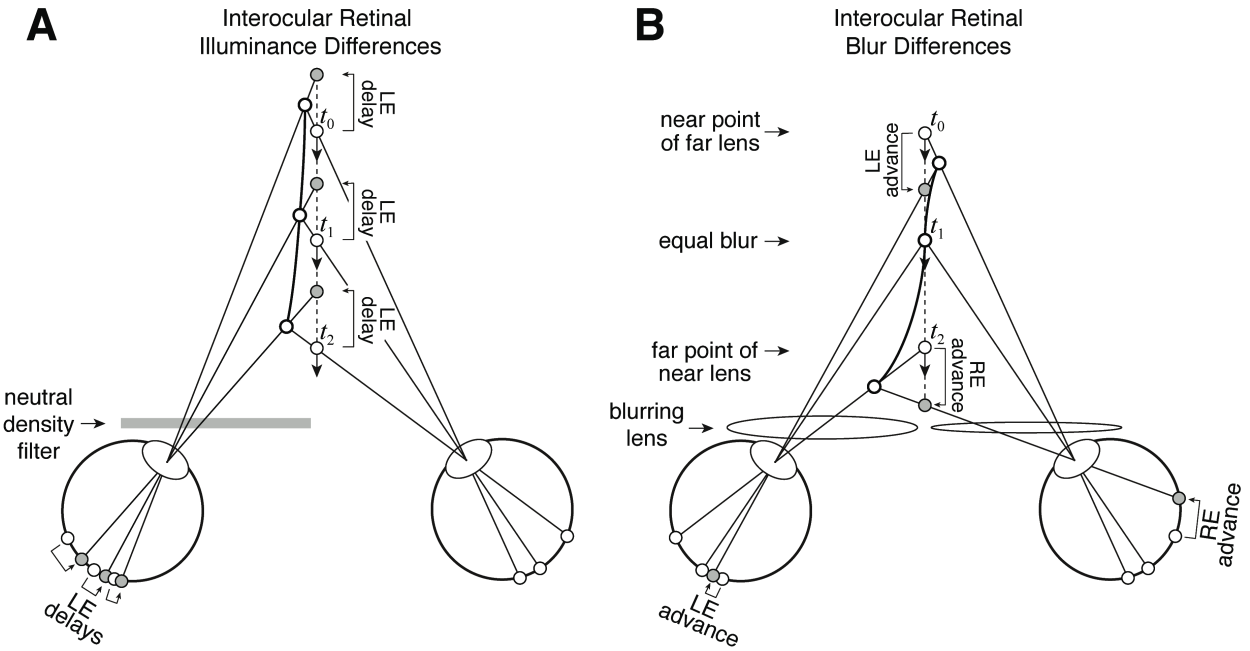

Figure S3. Misperception of motion towards the observer. Related to Figure 4. A Predicted perceived motion trajectory (bold curve), given target motion directly towards the observer (dashed line), with an interocular retinal illuminance difference. Here, a neutral density filter in front of the left eye causes its image to be processed more slowly, regardless of target distance. Stereo-geometry predicts that the target will appear to travel along a curved trajectory that bends towards the darkened eye (bold curve) rather than in a straight line[S2]. **B** Predicted perceived motion trajectory, given target motion directly towards the observer, with an interocular blur difference. The left eye is corrected for near and the right eye is corrected for far. The eye that is processed more quickly now changes systematically as a function of target distance. When the target is far, the left eye image will be blurry and be processed more quickly. When the target arrives at an intermediate distance where both eyes will form equally blurry images, the processing will be the same in both eyes and the target will appear to move directly towards the observer. When the target is near, the right eye image will be blurry and processed more quickly. The resulting illusory motion will trace an S-curve trajectory as the target traverses the distances between the near point of the far lens and the far point of the near lens. Even more striking effects occur for targets moving towards and to the side of the observer, along oblique motion trajectories. A full description of these effects, however, is beyond the scope of the current paper. (Note: the diagrams are not to scale.)

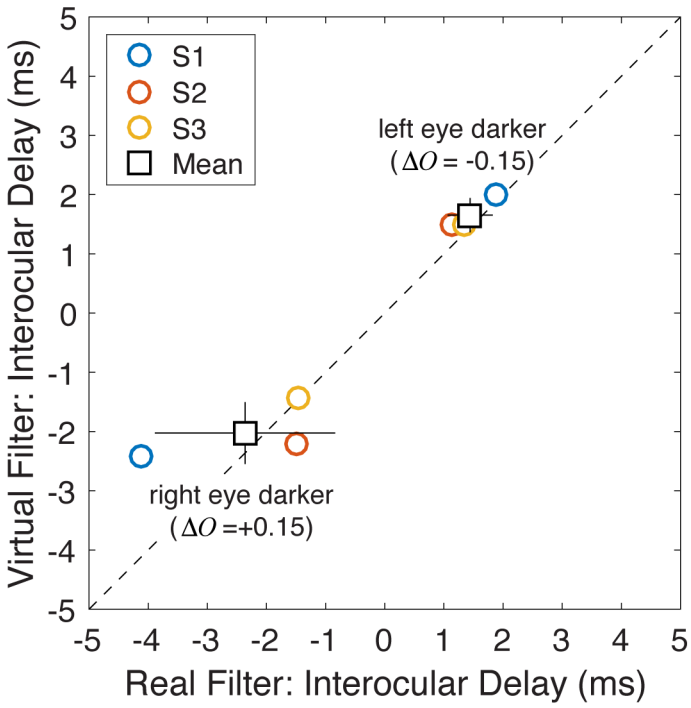

Figure S4. Real and virtual neutral density filters: Interocular delays. Related to STAR Methods-Neutral Density Filters. Real and virtual neutral density filters with the same optical densities (i.e. 0.15OD; 71% transmittance) caused similar delays for all human observers (colored circles) and the mean human observer (black square). Interocular differences in optical density, ΔO, are negative when the left eye retinal illuminance is reduced and positive when the right eye retinal illuminance is reduced. Error bars indicate standard deviations. The results suggest that the software implementation of the virtual neutral density filters was accurate.

Supplemental References

S1. Westheimer G, McKee SP. Stereoscopic acuity with defocused and spatially filtered retinal images. J Opt Soc Am A 1980;70:772–8.

S2. Spiegler JB. Apparent path of a pulfrich target as a function of the slope of its plane of notion. Am J Optom Physiol Opt 1986;63:209–16.